

Contributions of vehicular carbonaceous aerosols to PM_{2.5} in a roadside environment in Hong Kong

X. H. Hilda Huang¹, Q. J. Bian^{2,‡}, Peter K. K. Louie³ and Jian Zhen Yu^{1,2}

[1] {Institute for the Environment, Hong Kong University of Science & Technology, Clear Water Bay, Kowloon, Hong Kong}

[2] {Department of Chemistry, Hong Kong University of Science & Technology, Clear Water Bay, Kowloon, Hong Kong}

[3] {Hong Kong Environmental Protection Department, 47/F, Revenue Tower, 5 Gloucester Road, Wan Chai, Hong Kong}

[‡] {now at: Department of Atmospheric Science, Colorado State University, USA}

Correspondence to: J. Z. Yu (jian.yu@ust.hk)

Abstract

Hourly measurements of elemental carbon (EC) and organic carbon (OC) were made at Mong Kok, a roadside air quality monitoring station in Hong Kong for a year from May 2011 to April 2012. The monthly average EC concentrations were 3.8–4.9 $\mu\text{gC}/\text{m}^3$, accounting for 9.2–17.7% of the PM_{2.5} mass (21.5–49.7 $\mu\text{g}/\text{m}^3$). The EC concentrations showed little seasonal variation and peaked twice daily coinciding with the traffic rush hours of a day. Strong correlations were found between EC and NO_x concentrations, especially during the rush hours in the morning, confirming vehicular emissions as the dominant source for EC at this site. The analysis by the minimum OC/EC ratio approach to determine OC/EC ratio representative of primary vehicular emissions yields a value of 0.5 for (OC/EC)_{vehicle}. By applying the derived (OC/EC)_{vehicle} ratio to the dataset, the monthly average vehicle-related OC was estimated to account for 17–64% of the measured OC throughout the year. Vehicle-related OC was also estimated using receptor modeling of a combined dataset of hourly NO_x, OC, EC and volatile organic compounds characteristic of different types of vehicular emissions. The OC_{vehicle} estimations by the two different approaches were in good agreement. When both EC and vehicle-derived organic matter (OM) (assuming an OM-to-OC ratio of 1.4) are considered, vehicular carbonaceous aerosols contributed $\sim 7.3 \mu\text{g}/\text{m}^3$ to PM_{2.5}, accounting

31 for ~20% of PM_{2.5} mass (38.3 µg/m³) during winter when Hong Kong received significant
32 influence of air pollutants transported from outside and ~30% of PM_{2.5} mass (28.2 µg/m³)
33 during summertime when local emission sources were dominant. A reduction of 3.8 µg/m³ in
34 vehicular carbonaceous aerosols was estimated during 7:00–11:00 (i.e. rush hours on
35 weekdays) on Sundays and public holidays. This could mainly be attributed to less on-road
36 public transportation (e.g. diesel-powered buses) in comparison with non-holidays. These
37 multiple lines of evidence confirm local vehicular emissions as an important source of PM_{2.5}
38 in an urban roadside environment and suggest the importance of vehicular emission control in
39 reducing exposure to PM_{2.5} in busy roadside environments.

40

41 **1 Introduction**

42 Carbonaceous species is an important constituent of the PM_{2.5} (atmospheric particulate matter
43 with aerodynamic diameters less than 2.5 µm) (Seinfeld and Pandis, 1998) and a substantial
44 contributor to climate forcing, visibility impairment and adverse health effects (e.g. USEPA,
45 2004; IPCC, 2007). The carbonaceous material is commonly distinguished in elemental
46 carbon (EC) and organic carbon (OC). EC has an exclusive origin in primary emissions from
47 combustion of carbonaceous matter such as diesel, gasoline, biomass and organic wastes. In
48 particular, EC dominates the particle fraction of diesel engine exhaust, which has recently
49 been reclassified as carcinogenic to humans (e.g. USEPA, 2002; IARC, 2012). EC has been
50 considered to undergo little chemical transformation in the atmosphere, and thus it has been
51 used as an indicator for primary combustion emissions. OC can be directly generated from
52 primary emission sources (known as primary OC, POC) or formed through oxidation of
53 reactive organic gases followed by gas-to-particle conversion processes in the atmosphere
54 (known as secondary OC, SOC) (Gelencsér, 2004).

55 A significant fraction of PM_{2.5} mass, ranging from 16% in rural areas to around 40% in
56 urban/roadside areas, was identified as carbonaceous aerosols in Hong Kong (DRI, 2010;
57 HKUST, 2013). A clear regional-urban-street gradient from low to high in total carbon (TC)
58 concentrations has been consistently observed within Hong Kong during the past decade. The
59 higher EC concentrations at street level reflect the important contribution from traffic
60 emissions. While there exist a few studies examining the relative contributions of vehicular
61 emissions to the PM_{2.5} mass and its organic fraction in Hong Kong, fewer efforts have been
62 focused on roadside PM_{2.5} sources. Zheng et al. (2006) analyzed filter samples collected at
63 three contrasting sampling sites with respect to vehicular emission influence during 2000–

64 2001. They employed a chemical mass balance receptor model in combination with organic
65 tracers to apportion contribution of nine air pollution sources to PM_{2.5} OC. The contributions
66 to OC from vehicular emissions were reported to be approximately 70% at roadside site, 60%
67 at urban site and 25% at rural site. Guo et al. (2009) applied principal component analysis
68 with absolute principal component scores technique to the PM_{2.5} composition data obtained
69 from two one-year studies in Hong Kong and showed that vehicle emissions contributed
70 about 51%, 23% and 20% to the PM_{2.5} mass at roadside, urban site and rural site, respectively.
71 Hu et al. (2010) analyzed high-volume PM_{2.5} samples collected at four sites during the
72 summer of 2006 and used positive matrix factorization and chemical mass balance models to
73 apportion the source contributions to OC. The results showed that vehicular exhaust
74 contributed 41.0% and 8.4% to the ambient OC on sampling days that were mainly under the
75 influence of local emissions and regional transport, respectively. These source analysis
76 studies were all based on 24-hr filter measurements and they are inherently incapable of
77 capturing the dynamics of pollutant emissions and atmospheric chemical conversion
78 processes that happen on a faster time scale.

79 The Hong Kong Government has recognized the street-level air pollution as one of the most
80 important air pollution issues for Hong Kong and has taken a wide range of measures to
81 control the vehicular emissions (HKEPD, 2013). Hence, continuous efforts are in urgent need
82 to monitor PM_{2.5} components closely related to vehicular emissions and to estimate their
83 contributions to PM_{2.5} mass for the purpose of evaluating and formulating control measures
84 targeting lowering the roadside PM_{2.5}.

85 In this study, a semi-continuous thermal/optical carbon field analyzer was deployed at Mong
86 Kok (MK), one of the three roadside air quality monitoring stations (AQMS) in Hong Kong.
87 Mong Kok, with its extremely high population density of 130,000 persons per km², is
88 described as the busiest district in the world by the Guinness World Records. Measurements
89 of hourly OC and EC concentrations were conducted for a year from May 2011 to April 2012.
90 These high-time resolution OC and EC data were analyzed to examine their diurnal, weekly,
91 monthly and seasonal variations. The objectives are to derive the OC/EC ratio representing
92 primary vehicular emissions and to estimate the contributions of vehicular carbonaceous
93 aerosols to PM_{2.5} in the roadside environment in Hong Kong.

94

95

96 2 Experimental

97 2.1 Sampling equipment and method

98 A semi-continuous OC-EC field analyzer system (RT-3131, Sunset Laboratory, OR, USA)
99 was installed at MK AQMS, a roadside site located in a mixed residential and commercial
100 district in Hong Kong with heavy traffic and surrounded by many tall buildings. At the MK
101 AQMS, a few aerosol samplers are located on a platform around 3 m above the ground level
102 and instruments for the criteria gas pollutants are housed in a room at the site with their inlets
103 extending through the ceiling. The ECOC analyzer used in this work was located on the
104 ground with the inlet ~2 m above the ground and ambient air was drawn through a 2.5 μm
105 aerodynamic diameter cut point cyclone at a flow rate of 8 L/min. A carbon-impregnated
106 parallel plate organic denuder is placed upstream of the analyzer for removing gaseous
107 organics. The analyzer was programmed to collect particle samples for 46 min at the start of
108 each hour, followed by a 9-min sample analysis and 3-min instrument stabilizing process.

109 The thermal/optical analytical method is based on the modified National Institute for
110 Occupational Safety and Health (NIOSH) method 5040 protocol (Turpin et al., 1990; Birch
111 and Cary, 1996; NIOSH, 2003). During the thermal analysis, the sample deposited on the
112 quartz fiber filter is heated under different conditions and carbonaceous materials in the
113 sample are converted to CO_2 for detection by the non-dispersive infrared (NDIR) detector. In
114 the first stage, thermal ramping occurs in a helium (He) environment from room temperature
115 to 840°C to volatilize OC, followed by a brief cooling step to 550°C. In the second stage, the
116 carrier gas is switched to oxygen in helium (O_2/He) and the temperature is increased stepwise
117 to 870°C, oxidizing off all of the EC in the sample. The temperature profiles and purge gases
118 in each analysis stage is presented in Table S1 in the supplementary material. Since a fraction
119 of the OC could be pyrolyzed under the O_2 -free conditions, a tuned diode laser (660 nm) is
120 used to monitor the light transmission during the thermal analysis. In a typical analysis, the
121 laser transmittance signals first decreases due to the pyrolysis of OC, then it increases as the
122 pyrolyzed OC is oxidized in the presence of O_2 . When the laser signal returns to its initial
123 value at the beginning of the analysis, this sets the split point differentiating OC and EC.

124 Ultra-high purity grade gases (He, 10% O_2 in He and 5% CH_4 in He) were used. An O_2 trap
125 (SGT Middelburg V. V., the Netherlands) was installed in the He gas line to remove trace
126 amounts of O_2 . The quartz fiber filters were pre-baked inside the main oven of the instrument
127 at 870°C for about 5 min before sample collection and were replaced weekly.

128 In addition, hourly data including PM_{2.5} mass, NO, NO₂, and O₃ at the sampling site are
129 provided by the Hong Kong Environmental Protection Department (HKEPD).

130 **2.2 Quality control and data validation**

131 The semi-continuous carbon analyzer collected samples approximately 90% of the time
132 between May 1, 2011 and April 30, 2012. No data were collected during June 21–July 20,
133 2011 due to instrument maintenance and during August 23–30, 2011 due to malfunctioning
134 of NDIR.

135 The analyzer computer was closely monitored through a secured phone line and the
136 instrument was checked daily for any error flags for hardware or software problems. Weekly
137 routine instrument maintenance includes sample filter replacement, cyclone cleaning, one-
138 point external calibration, gas-flow and instrument blank checking. The instrument blank for
139 total carbon (TC) during the study period ranged from 0.02 to 0.25 µgC, with an average of
140 0.13 µgC. For the 1-hr measurement (46-min sampling at a flow rate of 8 L/min), the blank
141 values translate to 0.05–0.66 µgC/m³ (average of 0.35 µgC/m³) in atmospheric concentrations.
142 The method detection limits (MDLs), determined to be three times the blank standard
143 deviation, were 0.60 µgC/m³ for OC and 0.20 µgC/m³ for EC. Multi-point external
144 calibrations using known sucrose concentrations spiked on a prebaked filter were conducted
145 once every 1–2 months. Recommended by the manufacturer, 21.03 µgC was used for one
146 point calibration while 4.21, 21.03 and 42.07 µgC were used for multi-point calibration. The
147 recoveries of these three sucrose standard solutions were 119.0±8.4, 100.7±6.0 and
148 95.3±7.1%, respectively. When the organic denuder was changed once every two months, the
149 sampling flow rate calibration was performed and the actual flow rates were recorded within
150 8.0±0.4 L/min. Several experiments were conducted to determine the dynamic blank by
151 placing a 47-mm Teflon filter upstream of the denuder and sampling particle-free ambient air
152 into the analyzer on a 2-h collection/analysis cycle. The dynamic blank was in the range of
153 0.46–0.83 µgC/m³ with an average of 0.68 µgC/m³. The average dynamic blank corresponds
154 to 8.7% of the measured annual mean OC value. This value is consistent with the results from
155 previous studies (e.g. Polidori et al., 2006; Kang et al., 2010) and the finding from Turpin et
156 al. (1994) that the adsorption artifact is dependent on the concentrations of gaseous
157 OC/particulate OC. The volatilization of particulate OC from the sampling quartz fiber filter
158 was estimated to be 10±6% (upper limit) (Polidori et al., 2006). Considering that the positive
159 and negative artifacts are of comparable magnitude, no correction was made to the measured

160 OC concentrations in this study. The results from dynamic blank test serve as an estimate of
161 adsorption effect.

162 The data validation processes include checking of sampling volume, calibration peak area,
163 NDIR signals, and OCEC split point. Data with a sampled volume variation beyond the
164 tolerance of 5% (i.e., 368 ± 18 L) or a calibration peak area variation beyond the tolerance of
165 10% were considered to be invalid and excluded from the dataset. The raw data files of all the
166 collected samples were manually inspected to identify any abnormal OCEC split (i.e. the time
167 when the laser signal return to its initial value after the pyrolysis). In case of abnormal split,
168 the calculation software of the instrument was then used to process the raw data files with the
169 split point set manually. The data valid rate for the entire sampling period is 96%. The
170 effective sampling duration, data capture rates and valid rates for individual month are listed
171 in Table S2 in the supplementary material.

172 The semi-continuous OC and EC measurements (also abbreviated as RT measurements for
173 ease of discussion) were further validated by comparing with OC and EC data obtained from
174 two sets of off-line filter-based measurements. One is from the Hong Kong PM_{2.5} speciation
175 network program. In the speciation monitoring program, PM_{2.5} samples were collected on
176 prebaked 47-mm quartz fiber filters over a 24-h (starting from 0:00 at midnight) period by a
177 Partisol sampler (Rupprecht & Patachnick, Model 2025, NY, USA). The 24-h filter-based
178 measurements using the Partisol samplers, abbreviated as Partisol-TC, Partisol-OC and
179 Partisol-EC hereafter, were made every 6th day throughout the year. The other one is from the
180 PM_{2.5} organic speciation project. PM_{2.5} samples were collected on prebaked 20 × 25 cm
181 quartz fiber filters over a 24-h (starting from 0:00 at midnight) period by a High-Volume (HV)
182 PM_{2.5} particulate sampler (Tisch Environmental Inc., OH, USA) at a frequency of once every
183 three days. The HV sampler-derived measurements were abbreviated as HV-TC, HV-OC and
184 HV-EC hereafter. The sampled filters from both projects were stored in a freezer below –
185 20°C after collection and were analyzed using a lab-based thermal/optical carbon analyzer
186 (Sunset Laboratory, OR, USA). The ACE-Asia protocol (Schauer et al., 2003), a variant of
187 NIOSH protocol (Wu et al., 2012), was used for these 24-h filter samples. The hourly OC and
188 EC concentrations were averaged over the same 24-h period for comparison with the filter-
189 based concentrations. The comparisons are shown in Fig. 1.

190 The differences between the measurements were evaluated by zero-intercept linear regression,
191 average percent relative bias ($\% \overline{RB}$) and average percent relative standard deviation ($\% \overline{RSD}$).
192 The equations to calculate these two parameters are given in Appendix 1 in the

193 supplementary material. The instrument blanks for both the bench-top aerosol carbon
194 analyzer and the field OC-EC analyzer were statistically not different from zero after
195 considering the analytical and instrumental uncertainties of the blank. Hence, the zero-
196 intercept linear regression analysis was applied in the comparisons of the datasets.

197 TC by the semi-continuous method agrees reasonably well with both Partisol filter
198 measurements ($R^2 = 0.98$, $\% \overline{RB} = -29.6\%$, $\% \overline{RSD} = 23.4\%$) and high-volume filter
199 measurements ($R^2 = 0.99$, $\% \overline{RB} = -16.4\%$, $\% \overline{RSD} = 15.2\%$). Good correlations and
200 reasonable agreement were also observed for OC ($R^2 = 0.97$, $\% \overline{RB} = -33.8\%$, $\% \overline{RSD} = 27.7\%$
201 for RT-OC vs. Partisol-OC and $R^2 = 0.98$, $\% \overline{RB} = -17.9\%$, $\% \overline{RSD} = 18.4\%$ for RT-OC vs.
202 HV-OC). The average Y/X ratios were 0.75 ± 0.11 for RT-TC vs. Partisol-TC and 0.86 ± 0.11
203 for RT-TC vs. HV-TC, respectively. The Y/X ratios for RT-OC vs. Partisol-OC and RT-OC
204 vs. HV-OC were 0.72 ± 0.14 and 0.85 ± 0.18 , respectively. These numbers suggest that in
205 general both the TC and OC measurements from the off-line filter samples were larger than
206 those observed by the semi-continuous method. More specifically, the discrepancies were
207 larger between RT data and Partisol data than those between RT data and HV data. In
208 addition to the uncertainties associated with the sampling and analysis processes, another
209 possible reason is the positive artifacts due to organic vapor adsorption on the quartz fiber
210 filters since no denuder was used in either the Partisol or HV samplers. The amount of
211 organic vapor adsorbed onto the quartz fiber filter in the Partisol samplers was expected to be
212 higher than that in the HV samplers as the face velocity of the Partisol sampler is
213 approximately half of that of the HV sampler (McDow et al., 1990).

214 The EC data comparisons show a higher degree of scatter than TC and OC ($R^2 = 0.93$ for RT-
215 EC vs. Partisol-EC and $R^2 = 0.86$ for RT-EC vs. HV-EC) while the average Y/X ratios for EC
216 suggested that the semi-continuous data agree better with the filter-based measurements
217 (0.88 ± 0.26 for RT vs. Partisol samples and 1.04 ± 0.38 for RT vs. HV samples, respectively).
218 Several studies reported poor agreement between thermal EC from the field analyzer and
219 those filter-based EC measurements due to high detection limit and differences in the
220 temperature programs (e.g. Schauer et al., 2003; Bae et al., 2004; Venkatachari et al., 2006).
221 However, the discrepancies between RT-EC and filter-based EC measured at roadside in this
222 study might also be attributed to the different sampling durations. The field analyzer collected
223 $PM_{2.5}$ samples for a total of 1104 minutes on a daily basis, accounting for about 3/4 of the 24-
224 h period. The sampled air by the RT-OCEC analyzer might not be able to fully represent the

225 24-h integrated sampling period by the filter-based measurements because of the high carbon
226 concentrations with large variations at MK.

227

228 **3 Results and Discussions**

229 **3.1 Organic and elemental carbon concentrations**

230 The annual average OC and EC concentrations at MK AQMS during the study period were
231 7.8 and 4.4 $\mu\text{gC}/\text{m}^3$, respectively. The average OC and EC concentrations in individual
232 months and in different seasons during the study period are shown in Fig. 2. Based on the
233 local meteorological characteristics, the seasons were defined as follows: March 16–May 15
234 as spring; May 16–September 15 as summer; September 16–November 15 as fall and
235 November 16–March 15 of the next year as winter (Chin, 1986; Yuan et al., 2006).

236 OC had clear seasonal variation, with higher values in the winter months (Nov–Feb) and the
237 lowest values recorded in summertime (Jun–Aug). In comparison, EC exhibited little
238 seasonal variations, suggesting that it dominantly came from local emission sources. The
239 relative contributions of OC to $\text{PM}_{2.5}$ ranged from 15.5% (Jul. 2011) to 29.3% (Jan. and Feb.
240 2012) while EC percent contribution to $\text{PM}_{2.5}$ mass was the highest in summer (17.7% in Jun.
241 2011) and lowest in winter (9.2% in Dec. 2011). This can be explained by the quite
242 comparable EC concentrations throughout the year while $\text{PM}_{2.5}$ concentrations were much
243 lower during summertime than wintertime.

244 The weekly patterns showed that EC was elevated on weekdays and decreased to a minimum
245 on Sundays for all the months. OC also had the lowest values on Sundays compared to the
246 rest of the week but the variations were less distinct than those of EC. These patterns were
247 consistent with the traffic flow variation within a week and confirm vehicular sources as the
248 dominant contributor to EC while an important source for OC. For OC, unlike the EC
249 concentrations which maintained at a stable level during the study period, its concentrations
250 were evidently higher in winter months. The OC increment in winter over summer was
251 mainly attributed to air pollutants transported into the MK area from elsewhere if we consider
252 relevant OC and EC measurement data in Hong Kong reported for a wider spatial coverage.
253 A previous study examined PM_{10} EC and OC data in a monitoring network of nine general
254 stations and the MK roadside station across Hong Kong from 1998 to 2001 (Yu et al., 2004).
255 The winter average OC was found to be 5.7–10.5 $\mu\text{g}/\text{m}^3$ higher than the summer average OC

256 across the monitoring network, with the highest OC seasonal increment associated with the
257 station in the northernmost of the Hong Kong territory and the OC increment in MK (7.6
258 $\mu\text{g}/\text{m}^3$) similar to those recorded at a cluster of six general stations in the same airshed to the
259 south of Tai Mo Shan ($5.7\text{--}7.9 \mu\text{g}/\text{m}^3$). Such spatial variation characteristics strongly suggest
260 that the winter OC increment over the summer in Hong Kong was dominated by
261 regional/super-regional sources. This is also consistent with the seasonality of prevailing
262 background wind for Hong Kong, with northerly and northeasterly winds prevailing in winter
263 that bring more polluted air masses from mainland China (Yu et al., 2004). Although
264 additional local sources in winter, such as more of the semi-volatile cooking emissions
265 partitioning to the particle phase, could not be ruled out, their contributions to the winter OC
266 increment were most likely minor in comparison with outside sources.

267 The diurnal variations of carbon concentrations for weekdays (Mon–Fri), Saturdays, and
268 holidays (Sunday and public holidays) were examined for individual months (Fig. S1 & Fig.
269 S2) and four months were selected to represent the different seasons (Figures 3, August for
270 summer, October for fall, January for winter and March for spring). The EC concentrations
271 on holidays, especially during daytime, were consistently lower in individual months,
272 indicating the on-road diesel-powered vehicles as its major sources (i.e. reduced bus schedule
273 on holidays) and the “local” characteristics. The difference of OC concentrations between
274 weekdays and holidays was less significant in all seasons. The potential reasons include: (1)
275 more gasoline-powered vehicles (e.g. private cars) would offset the OC concentration
276 reduction due to fewer diesel-powered vehicles; (2) cooking-related activities might make
277 greater contributions during holidays, and (3) polluted air masses transported from elsewhere
278 outside Hong Kong make a more sizable contribution to OC, especially in winter and the two
279 transitional seasons (Yu et al., 2004), obscuring the weekday-holiday variation in primary OC
280 from vehicles.

281 The diurnal profiles for OC and EC also differ. EC concentrations started to increase from
282 7:00 in the morning and two peaks (7:00–11:00 and 16:00–19:00) were observed during the
283 day. These two periods of higher EC coincided with the rush hours in the city. EC
284 concentrations started to decrease around 19:00, and remained at a relatively low level from
285 midnight till the next early morning. NO_x and EC were found to correlate quite well with
286 each other especially during the time period of 9:00 pm–6:00 am (the next day) and the first
287 rush hour period (Fig. 4). In these two periods, the emission sources at roadside were
288 relatively limited and EC and NO_x would be primarily from vehicular exhaust. In contrast,

289 during the rest of the day, various emission sources for NO_x , together with the higher
290 reactivity of NO_x during daytime, could lead to a weaker correlation between NO_x and EC
291 concentrations.

292 The OC concentrations also peaked twice a day (11:00–16:00 and 19:00–22:00). The diurnal
293 profile comparison between OC and O_3 showed that one O_3 peak commonly appeared in the
294 early afternoon but was about 1–2 h earlier than the afternoon OC peak (Fig. 5). In the
295 roadside environment, the ozone concentration level was much lower due to titration by NO .
296 Nevertheless, an ozone peak appearing in the early afternoon was consistently observed in
297 different seasons (Fig. 5). Such a temporal characteristic tends to indicate that ozone could be
298 an indicator of photochemical processes even in a high NO roadside environment. In view of
299 the consistent observation of an ozone peak in the early afternoon, it is possible that the first
300 OC peak was related to secondary organic aerosol (SOA) formation. The nighttime OC peak,
301 on the other hand, could be associated with emissions from the larger number of mainly
302 gasoline-fuelled private cars on the road. In addition, the cooking-related activities possibly
303 also contribute to the higher OC levels during both of the time periods. We note that there
304 was the consistent presence of an early morning O_3 peak around 3–5 am local time in all
305 months. This nighttime ozone peak is also observed across all the urban monitoring sites in
306 Hong Kong. Integrated process analysis using chemical transport modeling (private
307 communication, Dr. Ying Li at HKUST) shows that vertical transport (advection and
308 diffusion) and NO_x titration are the major processes controlling nighttime O_3 abundance in
309 Hong Kong. The joint result of reduced NO_x titration and mixing-in of outside and upper air
310 masses, which contain higher O_3 concentrations, is thought to account for the early morning
311 O_3 peak that elevates to the level of background ambient air (< 20 ppb).

312 The different diurnal variations of OC and EC concentrations result in an OC/EC ratio pattern
313 of three peaks appearing during the day (Fig. S3). The first one is observed in the early
314 morning when EC concentrations were much lower than those of OC. The second peak
315 appeared in the early afternoon, coinciding with the first OC peak. The third peak was at
316 around 20:00 in the evening when the OC concentrations were high while EC concentrations
317 started to decrease.

318 **3.2 Estimation of the $(\text{OC}/\text{EC})_{\text{vehicle}}$**

319 The EC-tracer method, due to its simplicity, has long been used to estimate the relative
320 contributions of primary and secondary sources to measured particulate OC (e.g. Chu and

321 Macias, 1981; Wolff et al., 1982; Turpin et al., 1991; Turpin and Huntzicker, 1995; Cabada et
322 al., 2004; Plaza et al., 2006; Lonati et al., 2007; Yu et al., 2009). This method is based on the
323 assumption that EC is exclusively primary in origin and that EC and primary OC have
324 common emission sources (e.g. combustion, resuspension of combustion particles, etc.). The
325 measured OC concentration is the sum of POC and SOC:

$$326 \quad [OC]_{\text{measured}} = \text{POC} + \text{SOC} \quad (1)$$

327 POC is emitted mainly by combustion or combustion-related sources, but there might be also
328 a minor portion from non-combustion sources (e.g., biogenic sources), therefore,

$$329 \quad \text{POC} = [OC]_{\text{combustion}} + b \quad (2)$$

330 where b denotes non-combustion primary OC.

331 If an $(OC/EC)_{\text{pri}}$ representing the primary combustion sources at the measurement site is
332 known, POC can be calculated using the equation below:

$$333 \quad \text{POC} = \text{EC} \times (OC/EC)_{\text{pri}} + b \quad (3)$$

334 SOC can be subsequently derived as the difference between $[OC]_{\text{measured}}$ and POC, i.e., Eq (4).

$$335 \quad \text{SOC} = [OC]_{\text{measured}} - [\text{EC} \times (OC/EC)_{\text{pri}} + b] \quad (4)$$

336 Several approaches have been reported in the literature to estimate the $(OC/EC)_{\text{pri}}$, including
337 the use of (1) emission inventories of OC and EC from primary sources (*Gray et al.*, 1986);
338 (2) ambient OC and EC measurements made when primary source emissions are dominant
339 or/and when photochemical activities are weak (Turpin and Huntzicker, 1991); and (3) the
340 minimum OC/EC ratio obtained in the study period (Lim and Turpin, 2002). It is not a trivial
341 task to ensure that $(OC/EC)_{\text{pri}}$ determined in these approaches is representative of the
342 composite effect of multiple primary combustion sources, each having a time-varying
343 contribution to the ambient OC and EC. In addition, uncertainty in estimating b (see
344 discussion later in this section) introduces additional uncertainty in the estimates of POC and
345 SOC. While we recognize the difficulty in deriving reliable POC and SOC concentrations, by
346 comparison we see it is a much simpler task to derive an $(OC/EC)_{\text{vehicle}}$ ratio representative of
347 vehicular emissions for our roadside environment, since it has the unique characteristic of
348 vehicular emissions being the dominant EC source. Once $(OC/EC)_{\text{vehicle}}$ is determined,
349 OC_{vehicle} can be calculated using eq (5):

$$350 \quad OC_{\text{vehicle}} = \text{EC} \times (OC/EC)_{\text{vehicle}} \quad (5)$$

351 The approaches we use here in estimating $(OC/EC)_{\text{vehicle}}$ are the same as the last two
 352 approaches described above for $(OC/EC)_{\text{pri}}$. We first use a subset of data that have a given
 353 percentage of the lowest OC/EC ratios among the complete data set to derive $(OC/EC)_{\text{min}}$
 354 (Castro et al., 1999). The slope ($(OC/EC)_{\text{min}}$) and the intercept (b) in eq (3) were calculated
 355 by Deming regression of OC on EC using the lowest 5% data by OC-to-EC ratio. In the
 356 Deming regression analysis, the uncertainties in both x- and y-axes are taken into account
 357 (Deming, 1943; Cornbleet and Gochman, 1979). Deming regression has been shown to have
 358 better performance in the EC tracer method than the ordinary least-square (OLS) regression,
 359 which only considers random measurement errors in y (Chu et al., 2005; Saylor et al., 2006).

360 There are different forms of Deming regression because of different ways of representing
 361 measurement errors in x and y, i.e. $\omega(X_i)$ and $\omega(Y_i)$ in eq (6) for S , which is the sum of the
 362 square of the perpendicular distances between the data points and the regression line (Saylor
 363 et al., 2006).

$$364 \quad S = \sum[\omega(X_i)(x_i - X_i)^2 + \omega(Y_i)(y_i - Y_i)^2] \quad (6)$$

365 In eq (6), X_i and Y_i are the observed data points and x_i and y_i are the adjusted points lying on
 366 the regression line. The simplest form of Deming regression, termed default Deming
 367 regression, adopts a value of 1 for λ , the ratio of $\omega(X_i)$ and $\omega(Y_i)$ (eq (7)). In another words,
 368 equal measurement uncertainties for variable X_i and Y_i are assumed.

$$369 \quad \lambda = \omega(X_i)/\omega(Y_i) \quad (7)$$

370 Saylor et al. (2006) compared two forms of Deming regression, default Deming regression
 371 with $\lambda = 1$ and optimal Deming regression with an accurate representation of
 372 λ (i.e., $\lambda = \text{Var}(\varepsilon_{OC})/\text{Var}(\varepsilon_{EC})$, where $\text{Var}(\varepsilon)$ is the variance of the measurement errors,
 373 ε). Using simulated EC and OC data, they demonstrated that the optimal Deming regression
 374 provides excellent results while the default Deming regression yields a slope of 6% larger
 375 than the true value and a negative intercept of -1.28 due to inaccurate representation of error
 376 variance. We therefore adopt optimal Deming regression in our linear regression approach to
 377 calculate $(OC/EC)_{\text{min}}$, and λ is taken to be the ratio of the measurement error variance of X
 378 and Y .

379 The regressions were performed on a monthly, seasonal and annual basis so as to evaluate the
 380 robustness of different subsets of data and the results are shown in Table 1. It is noted that
 381 some intercept values are negative, which does not seem to have a physical basis. To

382 understand the issue of negative intercepts, we next examine regression lines obtained with
383 OLS, default Deming, and optimal Deming regression for the January 2012 data (Fig. S4),
384 which had the largest negative intercept (-0.58) among all the monthly $(OC/EC)_{min}$. The OLS
385 regression results in a positive intercept (0.86) while the two Deming regressions give
386 negative intercepts. The different regression lines are apparently a result of difference in
387 assigning weights to individual observations. This result suggests that the regression line
388 intercept is fairly sensitive to weights assigned to individual observations, or in another word,
389 error variances for X and Y variables. For actual ambient data, it is difficult to identify a
390 subset of data that is free of SOC contribution or such a subset of data simply does not exist.
391 In addition, multiple primary combustion sources that have different $(OC/EC)_{pri}$ co-exist and
392 their relative strengths vary with time at a given ambient location. Both factors would
393 contribute to scattering of the data that are used for deriving $(OC/EC)_{pri}$, which in turn could
394 lead to a negative intercept, as illustrated by Fig. S4. This analysis about intercept shows the
395 large uncertainty associated with the estimated b when using linear regression approaches.
396 One needs to be cautious in estimating POC and SOC if a linear regression approach is relied
397 upon for the calculation of non-combustion-derived primary OC (i.e., b in eqs. (3) and (4)).
398 On the other hand, we note the slope is much less sensitive to different regression approaches.
399 In the example of the January 2012 data, the slope values derived from the two Deming
400 regressions differ less than 5% (Fig. S4). This adds to our confidence in the robustness of the
401 derived $(OC/EC)_{min}$ using Deming regression of select ambient OC and EC data.

402 The monthly $(OC/EC)_{min}$ values derived using the lowest 5% data by OC-to-EC ratio
403 exhibited lower values during summer months. In particular, the value was 0.38 in July and
404 0.52 in August. Higher values of $(OC/EC)_{min}$ were observed for December 2011 (1.46) and
405 January 2012 (1.42). The monthly variations of $(OC/EC)_{min}$ are consistent with the
406 estimations for different seasons. The lowest value (0.49) was found in summer, which is a
407 season mainly under the influence of local primary emissions and from time to time the
408 southerly winds from the ocean would bring in cleaner air to further dilute the pollution in
409 Hong Kong. During winter season, the prevailing winds were northerly and northeasterly and
410 the regional transport of air pollutants played a significant role (Yu et al., 2004). The higher
411 $(OC/EC)_{min}$ ratio is a combined result of primary sources having higher (OC/EC) and non-
412 negligible contribution of SOA in the 5% lowest (OC/EC) samples. Spring and fall are
413 transitional seasons with prevailing winds as a combination of southerly and northerly and
414 therefore the $(OC/EC)_{min}$ values were recorded to be in-between.

415 Since local primary emission sources are dominant during summertime, additional Deming
416 regressions were performed on the summer OC and EC dataset by varying the percentage of
417 included data from the lowest 5% to 100% (Table 2). The regression slope gradually
418 increases from 0.49 when the lowest 5% data ($n = 94$) are used for regression to 1.21 as all
419 summer data ($n = 1878$) are included for regression. The summer data and the Deming
420 regression lines are shown in Fig. S5. Based on this Deming regression analysis for this
421 “local emissions-influenced” period, a value of 0.5 was suggested to approximate
422 $(OC/EC)_{\text{vehicle}}$ while 1.2 could serve as an upper limit of $(OC/EC)_{\text{vehicle}}$ estimate at this
423 roadside site.

424 To evaluate the impact of different emission sources on the OC/EC ratio, we further
425 examined the OC/EC ratios in subsets of data selected according to the carbon diurnal
426 profiles. Three time periods were chosen; including two EC peak times (7:00–11:00 in the
427 morning and 16:00–19:00 in the afternoon) and one OC peak time (19:00–22:00 in the
428 evening). The appearance of EC peaks in the daytime and OC peak in the evening time
429 reflected enhancement of primary emissions during these periods. Hence, the OC/EC ratios in
430 these time periods were more influenced by primary emissions. Table 3 lists the average
431 OC/EC ratios, calculated as the average OC to the average EC, in the three time periods in
432 individual months. We note that data from the identified episodic periods, defined to be
433 periods when the hourly $PM_{2.5}$ mass concentrations exceeded the monthly average plus one
434 standard deviation for 4 hours or more, were excluded since on episode days the carbon
435 concentrations were considerably influenced by more aged air masses transported from
436 outside-Hong Kong.

437 The average OC/EC ratio for the same time period varied with months. Higher values were
438 observed in fall and winter months while lower in summer months (May–September). This is
439 consistent with the hypothesis that local sources dominated in summertime while transported
440 air masses largely impacted Hong Kong during winter leading to higher OC/EC ratios.

441 Within the same month, the OC/EC ratios in the two EC peak periods were mostly
442 comparable and 4-40% higher in the second EC peak periods, and both periods were lower
443 than that in the period of 19:00–22:00. This is expected since the first two periods were
444 dominated by vehicular emissions. During these two rush-hour periods of the day, public
445 transportation (e.g. buses, light buses, good vehicles, etc.) were predominant on the road and
446 most of them were diesel-powered vehicles. During evening time, more private cars, which
447 were predominately powered by gasoline engines, were on the road. The OC/EC ratios, as

448 reported in source profile studies, were 0.6–0.8 for diesel engine exhaust, 2.2–4.2 for
449 catalyst-equipped gasoline exhaust, and 8.2–60.0 for noncatalyst gasoline-powered exhaust
450 (Hildemann *et al.*, 1991; Schauer *et al.*, 1999a, 2002a). The compositional variation in the on-
451 road motor vehicles is expected to result in different OC/EC ratios. The average OC/EC
452 ratios in the 19:00–22:00 were 46–82% higher than those in the 16:00–19:00 periods in
453 different months. The elevation of OC relative to EC in the 19:00–22:00 could not possibly
454 come from SOC, as the SOC contribution would be expected to be higher in the 16:00–19:00
455 period which was partly daytime. In view of the site in a district of numerous restaurants, the
456 consistently higher OC/EC during 19:00–22:00 was most likely caused by cooking-related
457 activities. Work on cooking source samples revealed that little EC was emitted from cooking
458 while OC accounted for 34–69% of the emitted PM_{2.5} mass (Hildemann *et al.*, 1991; Schauer
459 *et al.*, 1999b, 2002b). This primary OC source from cooking would certainly increase the
460 ambient OC/EC ratios.

461 The comparisons between the calculated (OC/EC)_{min} values using all data versus the average
462 OC/EC in subsets of the data under significant influence of primary emissions clearly show
463 the difficulty in deriving a single (OC/EC)_{pri} value to represent a composite of multiple
464 primary sources, since each source makes time-varying contributions. It can also be seen that
465 using the (OC/EC)_{min} to represent the primary OC/EC ratio in the EC-tracer method would
466 lead to overestimation of SOC during time periods when cooking-related sources were
467 significant. Partly for this reason, we did not attempt to estimate POC and SOC in this study.
468 On the other hand, the accumulative evidence suggests that it is reasonable to adopt a value
469 of 0.5, the (OC/EC)_{min} value derived from Deming regression of the 5% lowest summer data
470 by OC-to-EC ratio, to approximate the OC/EC ratio for vehicular emissions. With EC at this
471 location is predominantly from vehicular emissions, the vehicle-related OC (i.e., OC_{vehicle}) is
472 then $0.5 \times EC$. We note OC_{vehicle} estimated in this way only accounts for primary OC
473 emission from vehicles. SOC formed from volatile organic compound (VOC) precursors
474 emitted by vehicles (e.g., toluene) is not captured in this EC tracer approach.

475 **3.3 Estimation of vehicle-related OC and PM_{2.5}**

476 **3.3.1 Estimation using (OC/EC)_{vehicle} inferred from OCEC measurements**

477 The annual average vehicle-related OC (OC_{vehicle}) concentration was $2.2 \pm 1.2 \mu\text{gC}/\text{m}^3$, which
478 represents $32.0 \pm 18.9\%$ of the annual average particulate OC. The monthly average OC_{vehicle}

479 concentrations showed little variation throughout the year ($1.9\text{--}2.4\ \mu\text{gC}/\text{m}^3$) while the percent
480 contribution to total OC varied from 16.6% in December to 64.0% in July. By applying a
481 ratio of 1.4 to convert OC to organic matter (OM) (Malm et al., 1994), the daily-average
482 contributions of vehicle-related organic aerosols ($\text{OM}_{\text{vehicle}}$) to the $\text{PM}_{2.5}$ mass were estimated
483 to be in the range of 3.5–24.8%. By further summing up the concentrations of $\text{OM}_{\text{vehicle}}$ and
484 EC, the vehicle-related carbonaceous $\text{PM}_{2.5}$ ($\text{PM}_{\text{vehicle}}$) and its contributions to the $\text{PM}_{2.5}$ mass
485 can be estimated. The monthly average $\text{PM}_{\text{vehicle}}$ ranged from 6.5 to $8.3\ \mu\text{gC}/\text{m}^3$ and exhibited
486 little seasonal variations (Fig. 6), reflecting the local nature of vehicular emission source. Its
487 relative contributions to the total $\text{PM}_{2.5}$ mass, on the other hand, varied from 16.0% (Dec.
488 2011) to 35.6% (Aug. 2011) with an annual average of 24.8%. The percent contribution
489 differences were mainly due to higher $\text{PM}_{2.5}$ levels during winter time. Calculations also
490 show that the average $\text{PM}_{\text{vehicle}}$ concentrations were estimated to be $10.3\ \mu\text{g}/\text{m}^3$ during the
491 first rush hour period (7:00–11:00) on non-holidays and $6.5\ \mu\text{g}/\text{m}^3$ for the same period on
492 holidays (including Sundays and public holidays). Hence, a reduction of approx. 37% in
493 $\text{PM}_{2.5}$ mass for the period of 7:00–11:00 on holidays could be attributed to reduction in
494 vehicular emissions, which is a result of reduced on-road public transportation (e.g. diesel-
495 powered buses). On Sundays and public holidays, bus frequencies decrease by 20–30%
496 compared to the rest of the week. These results indicate that the emissions from on-road
497 vehicles are an important source of $\text{PM}_{2.5}$ in the urban roadside environment of Hong Kong.

498 **3.3.2 Estimation using receptor modeling analysis**

499 The $\text{OC}_{\text{vehicle}}$ were also estimated by a receptor modeling approach so that comparisons can
500 be conducted for evaluation of the EC tracer method. In the receptor modeling approach,
501 source apportioning was performed on OC and EC by Positive Matrix Factorization (PMF)
502 Model. The input data consist of hourly concentrations of 27 volatile organic compounds
503 (VOCs), NO, NO_2 , OC and EC. The VOC measurements were conducted on an hourly/half-
504 hourly basis using a GC955 series 611/811 VOC analyzer (Syntech Spectras, Netherlands) at
505 MK AQMS. Isoprene was excluded from the input dataset since the biogenic emissions at
506 roadside can be neglected. *Iso*-hexane was also excluded as >30% of its measurements were
507 below the method detection limit.

508 The uncertainties for individual species were initially estimated as $(s_{ij} + \text{MDL}_{ij}/3)$ (e.g.,
509 Polissar et al., 1998; Reff et al., 2007), where MDL_{ij} is the method detection limit and s_{ij} is
510 the analytical uncertainty of the corresponding species in the data set. The analytical

511 uncertainties were assumed to be 10% of the species concentrations for most of the VOCs
512 and 5% for NO and NO₂. The smaller molecules (i.e. ethane, ethane and ethyne) coelute in
513 the GC analysis, causing larger uncertainties. A few VOCs (e.g. 1,3,5- and 1,2,3-
514 trimethylbenzenes, butenes and pentenes) were detected in less than 90% of the samples. The
515 uncertainties of these VOCs were increased by a factor of 3 in the PMF analysis. For data
516 which are below the detection limits, the concentrations were replaced with the value
517 ($MDL_{ij}/2$) and the corresponding uncertainty was set to $((5/6) \times MDL_{ij})$ (Polissar et al., 1998).

518 The source apportioning modeling was performed using EPA PMF 3.0 software (available at
519 <http://www.epa.gov/heads/research/pmf.html>). This software provides the bootstrap model
520 which is based on the Monte Carlo principle to check the mathematical stability of selected
521 runs (Norris et al., 2008). Each modeling run included 20 base runs and the base run with the
522 minimum Q value was retained as the solution. Solutions for 4–9 factors were tested and the
523 six-factor solution was considered to be the reasonable one. The source profiles of the six-
524 factor solution are shown in Fig. 7.

525 The first factor is rich in ethane, ethyne and benzene, all of which are relatively stable species.
526 This factor is therefore associated with aged air mass, which was transported from other
527 places. During the aging processes, reactive compounds such as alkenes would decay more
528 rapidly than unreactive species and the oxidative state of the aerosols would be increased.
529 The OC/EC ratio in this source profile was higher than 2, consistent with the nature of aged
530 air mass.

531 The second, third and sixth factors are all identified as vehicular emissions from diesel-
532 powered and gasoline-powered engines. Factor 2 is proposed to be dominated by diesel
533 exhaust as it is characterized by the presence of 1,3,5-trimethylbenzene, 1,2,4-
534 trimethylbenzene and 1,2,3-trimethylbenzene. The three VOC species appear in the distinct
535 source profile of Hong Kong diesel fuel, as reported by Tsai et al. (2006). In particular, this
536 factor is associated with the lowest OC/EC ratio (0.44) among all the factors, together with a
537 large amount of NO. These characteristics strongly suggest the association of this factor with
538 freshly emitted diesel exhaust. Factor 3 is dominated by *i*-pentane, *n*-pentane, pentenes and
539 three trimethylbenzenes. Since pentanes have been reported as markers of gasoline vapors in
540 Hong Kong (Tsai et al., 2006) and the OC/EC ratio in this factor (1.13) is higher than that in
541 factor 2, it is suggested that the third factor represents the better mixed air mass. Factor 6 is
542 related to gasoline-powered engine exhaust, characterized by the presence of *i*-pentane which
543 is the major component in gasoline vapor, and *cis*-2-butene and 1,3-butadiene which are two

544 common indicators for vehicle exhaust. The OC/EC ratio in this factor (2.36) is higher than
545 those in the other two factors.

546 The fourth factor is distinguished by a large amount of toluene, benzene, ethylbenzene,
547 xylenes, C₆ and C₇ alkanes. This source is considered to be a composite of emissions from
548 solvent use, architectural paints and industrial activities (Seila et al., 2001; Chan et al., 2006).
549 The industrial and architectural sources are an important source of aromatic VOCs, but they
550 make limited contributions to particulate OC and EC at MK.

551 The fifth factor is dominated by propane, *i*-butane and *n*-butane, hence is identified as the
552 emissions from the use of liquefied petroleum gas (LPG) in vehicles, gas stations and
553 cooking activities (Blake and Rowland, 1995). It is noted that LPG combustion and vapors
554 barely contributed to the carbon fraction in PM_{2.5} since the light alkanes emitted from LPG
555 are too volatile to reside in the particle phase.

556 On the basis of the source identifications, OC apportioned into factors 2, 3, 5 and 6 were
557 summed up to represent the PMF-derived OC_{vehicle}. The comparison of daily OC_{vehicle}
558 obtained from the EC-tracer method and the PMF approach is shown in a time series plot (Fig.
559 8). A fairly good agreement was observed between the estimations from the two methods (R^2
560 = 0.96). On average, PMF-derived OC_{vehicle} were approximately 25% higher than those
561 calculated by the EC-tracer method. The discrepancies could be due to one or a combination
562 of the following reasons: 1) uncertainties of the PMF analysis; 2) uncertainty in the
563 (OC/EC)_{vehicle} caused by the variation of the vehicle composition and 3) omission of the
564 cooking-related OC.

565 The relative contributions of different vehicular emission sources to the OC_{vehicle} and EC were
566 estimated by the PMF approach (Fig. 8, pie charts). The diesel-dominant factor (Factor 2)
567 contributed the most to EC and approximately one third to OC_{vehicle}. The gasoline-dominant
568 factor (Factor 6) contributed the least to EC but the most to OC_{vehicle}. These estimations
569 indicate that both diesel-powered and gasoline-powered vehicles are significant contributing
570 sources to the carbonaceous particle levels at roadside.

571

572 **4 Conclusions**

573 PM_{2.5} carbon measurements of hourly time resolution were conducted in the roadside
574 environment of Hong Kong for the first time, over a 12-month period from May 2011 to
575 April 2012. Three levels of validation were performed and the data valid rate for the entire

576 sampling period is approximately 96%. The OC and EC concentrations at MK AQMS during
577 the study period were on average 7.8 and 4.4 $\mu\text{gC}/\text{m}^3$, respectively. Higher OC
578 concentrations were recorded during winter months as a result of the contributions of regional
579 air pollutant transport. EC concentrations were comparable among individual months. In
580 addition, the EC concentrations peaked in two time periods which coincided with the traffic
581 rush hours of a day. Both results indicate that EC was dominantly emitted from local
582 vehicular sources.

583 The minimum OC/EC ratios for periods of elevated EC were derived using Deming
584 regression. The results indicated that using a single value to represent $(\text{OC}/\text{EC})_{\text{pri}}$ for the
585 purpose of estimating POC and SOC by the EC-tracer method may cause significant biases
586 since there were multiple significant primary emission sources in the sampling area, each
587 making time-varying contributions. On the other hand, a value of 0.5, mainly based on OC
588 and EC measurements in the lowest 5% by OC-to-EC ratio in the summer during which local
589 emissions dominated as a result of prevailing meteorological conditions, can be proposed to
590 reasonably approximate the OC/EC ratio for primary vehicular emissions. The annual
591 average vehicle-related OC concentration was subsequently estimated to be $2.2 \pm 1.2 \mu\text{gC}/\text{m}^3$,
592 which accounted for $32.0 \pm 18.9\%$ of the total $\text{PM}_{2.5}$ OC. The monthly average $\text{OC}_{\text{vehicle}}$
593 concentrations had a small variation throughout the year ($1.9\text{--}2.4 \mu\text{gC}/\text{m}^3$) while its
594 contribution to total OC varied from 16.6% (December 2011) to 64.0% (July 2011). The
595 $\text{OC}_{\text{vehicle}}$ derived from source apportionment analysis by PMF are in good agreement with the
596 estimates using the proposed $(\text{OC}/\text{EC})_{\text{vehicle}}$, adding confidence to the estimated primary OC
597 contribution from the vehicular source. Assuming an OM-to-OC ratio of 1.4, the daily-
598 average contributions of $\text{OM}_{\text{vehicle}}$ to $\text{PM}_{2.5}$ ranged from 3.5 to 24.8%. The annual average
599 concentration of $\text{PM}_{\text{vehicle}}$ was estimated to be $7.4 \mu\text{g}/\text{m}^3$ and accounted for approx. 25% of
600 the $\text{PM}_{2.5}$ concentration, confirming vehicular emissions as an important source of $\text{PM}_{2.5}$
601 mass.

602 The carbon diurnal profiles also suggest cooking-related activities as an important primary
603 source to OC in the study area, making it difficult relying on the EC tracer method to estimate
604 the relative contributions of POC and SOC. Higher resolution measurements of particle-phase
605 tracer compounds for the cooking sources (e.g. C_{16} and C_{18} fatty acids) and for the vehicle-
606 related SOA (e.g., phthalic acid) in conjunction with receptor modeling could provide
607 possibilities in a more accurate estimation of SOA contributions in the urban areas of Hong
608 Kong.

609

610 **Acknowledgements**

611 This work is supported by the Hong Kong Environmental Protection Department (HKEPD)
612 (Tender Ref. AS 10-336) and the Environment and Conservation Fund/Woo Wheelock Green
613 Fund (ECWW09EG04). We thank HKEPD for provision of the real-time PM_{2.5} and VOC
614 datasets. Special thanks go to Dr. Damgy H. L. Chan of HKEPD for her many inputs, her
615 tireless efforts in gathering a voluminous amount of the real-time VOC data, and assistance in
616 sampling logistics. The content of this paper does not necessarily reflect the views and
617 policies of the HKSAR Government, nor does mention of trade names or commercial
618 products constitute an endorsement or recommendation of their use.

619

620 **References**

- 621 Bae, M. S., J. J. Schauer, J. T. DeMinter, J. R. Tunner, D. Smith, and R. A. Cary: Validation of a
622 semi-continuous instrument for elemental carbon and organic carbon using a thermal-optical method,
623 *Atmos. Environ.*, 38, 2885-2893, 2004.
- 624 Birch, M. E. and R. A. Cary: Elemental carbon-based method for monitoring occupational exposures
625 to particulate diesel exhaust, *Aerosol Sci. Technol.*, 25, 221-241, 1996.
- 626 Cabada, J. C., S. N. Pandis, R. Subramanian, A. L. Robinson, A. Polidori, and B. Turpin: Estimating
627 the secondary organic aerosol contribution to PM_{2.5} using the EC tracer method, *Aerosol Sci. Technol.*,
628 38, 140-155, 2004.
- 629 Castro, L. M., C. A. Pio, R. M. Harrison, and D. J. T. Smith: Carbonaceous aerosol in urban and rural
630 European atmospheres: estimation of secondary organic carbon concentrations, *Atmos. Environ.*, 33,
631 2771-2781, 1999.
- 632 Chan, L. Y., K. W. Chu, S. C. Zou, C. Y. Chan, X. M. Wang, B. Barletta, D. R. Blake, H. Guo, and W.
633 Y. Tsai: Characteristics of nonmethane hydrocarbons (NMHCs) in industrial, industrial-urban, and
634 industrial-suburban atmospheres of the Pearl River Delta (PRD) region of South China, *J. Geophys.*
635 *Res.*, D11304, doi:10.1029/2005JD006481, 2006.
- 636 Chin, P. C.: Climate and weather, *A Geography of Hong Kong*, edited by Chiu, T. N. and C. L. So,
637 Oxford University Press, New York, 69-85, 1986.
- 638 Chu, L. C. and E. S. Macias: Carbonaceous urban aerosol - primary or secondary? in *Atmospheric*
639 *Aerosol Source Air Quality Relationships*, edited by Macias, E. S. and P. K. Hopke, pp. 251-268,
640 1981.

641 Chu, S. -H.: Stable estimate of primary OC/EC ratio in the EC tracer method, *Atmos. Environ.*, 39,
642 1383-1392, 2005.

643 Cornbleet, P. J. and N. Gochman: Incorrect least-squares regression coefficients, *Clin. Chem.*, 25,
644 432-438, 1979.

645 Deming, W. E.: *Statistical adjustment of data*, Wiley, NY, USA, 1943.

646 DRI (Desert Research Institute): Measurements and validation for 2008/2009 particulate matter study
647 in Hong Kong, 2010, PM_{2.5} speciation study in Hong Kong, available at:
648 [http://www.epd.gov.hk/epd/english/environmentinhk/air/study/rpts/files/HKEPDPDFinalReportRev_11-](http://www.epd.gov.hk/epd/english/environmentinhk/air/study/rpts/files/HKEPDPDFinalReportRev_11-29-10_v2.pdf)
649 [29-10_v2.pdf](http://www.epd.gov.hk/epd/english/environmentinhk/air/study/rpts/files/HKEPDPDFinalReportRev_11-29-10_v2.pdf), 2010.

650 Gelencsér, A.: *Carbonaceous Aerosol*, Springer, Netherlands, 2004.

651 Gray, H. A., G. R. Cass, J. J. Huntzicker, E. K. Heyerdahl, and J. A. Rau: Characteristics of
652 atmospheric organic and elemental carbon particle concentrations in Los-Angeles, *Environ. Sci.*
653 *Technol.*, 20, 580-589, 1986.

654 Guo, H., A. J. Ding, K. L. So, G. Ayoko, Y. S. Li, and W. T. Hung: Receptor modeling of source
655 apportionment of Hong Kong aerosols and the implication of urban and regional contribution, *Atmos.*
656 *Environ.*, 43, 1159-1169, 2009.

657 Hildemann, L. M., G. R. Markowski, and G. R. Cass: Chemical composition of emissions from urban
658 sources of fine organic aerosol, *Environ. Sci. Technol.*, 25, 744-759, 1991.

659 Hu, D., Q. Bian, A. K. H. Lau, and J. Z. Yu: Source apportioning of primary and secondary organic
660 carbon in summer PM_{2.5} in Hong Kong using positive matrix factorization of secondary and primary
661 organic tracer data, *J. Geophys. Res.*, 115, D16204, doi:10.1029/2009JD012498, 2010.

662 HKEPD (Environmental Protection Department, the Government of the HKSAR): Hong Kong's
663 Environment, available at:
664 http://www.epd.gov.hk/epd/english/environmentinhk/air/air_maincontent.html, 2013.

665 HKUST (the Hong Kong University of Science & Technology): Measurements and validation for the
666 twelve-month particulate matter study in Hong Kong, 2012, PM_{2.5} speciation study in Hong Kong,
667 available at:
668 [http://www.epd.gov.hk/epd/english/environmentinhk/air/study/rpts/files/final_report_mvtmpms_2012.](http://www.epd.gov.hk/epd/english/environmentinhk/air/study/rpts/files/final_report_mvtmpms_2012.pdf)
669 [pdf](http://www.epd.gov.hk/epd/english/environmentinhk/air/study/rpts/files/final_report_mvtmpms_2012.pdf), 2013.

670 IARC (International Agency for Research on Cancer): IARC monographs on the evaluation of
671 carcinogenic risks to humans, volume 105: Diesel and gasoline engine exhausts and some nitroarenes,

672 World Health Organization (WHO), United Nations (UN), available at: [http://www.iarc.fr/en/media-](http://www.iarc.fr/en/media-centre/pr/2012/pdfs/pr213_E.pdf)
673 [centre/pr/2012/pdfs/pr213_E.pdf](http://www.iarc.fr/en/media-centre/pr/2012/pdfs/pr213_E.pdf), 2012.

674 IPCC (Intergovernmental Panel on Climate Change): Climate Change 2007 (AR4): The Physical
675 Science Basis, Cambridge University Press, UK, 2007.

676 Kang, C. -M., P. Koutrakis, and H. H. Suh: Hourly measurements of fine particulate sulfate and
677 carbon aerosols at the Harvard-U.S. Environmental Protection Agency Supersite in Boston, *J. Air*
678 *Waste Manag. Assoc.*, 60, 1327-1334, 2010.

679 Lim, H. J. and B. J. Turpin: Origins of primary and secondary organic aerosol in Atlanta: results of
680 time-resolved measurements during the Atlanta supersite experiment, *Environ. Sci. Technol.*, 36,
681 4489-4496, 2002.

682 Lonati, G., S. Ozgen, and M. Giugliano: Primary and secondary carbonaceous species in PM_{2.5}
683 samples in Milan (Italy), *Atmos. Environ.*, 41, 4599-4610, 2007.

684 Malm, W. C., J. F. Sisler, D. Huffman, R. A. Eldred, and T. A. Cahill: Spatial and seasonal trends in
685 particle concentration and optical extinction in the United States, *J. Geophys. Res.*, 99, 1347-1370,
686 1994.

687 McDow, S. R. and J. J. Huntzicker: Vapor adsorption artifact in the sampling of organic aerosol: face
688 velocity effects, *Atmos. Environ.*, 24A, 2563-2571, 1990.

689 NIOSH: Monitoring of diesel particulate exhaust in the workplace, Third supplement to Manual of
690 Analytical Methods, 4th Edition, Cincinnati, OH. Publication No. 2003-154, 2003.

691 Ogren, J. A. and R. J. Charlson: Elemental carbon in the atmosphere: cycle and lifetime, *Tellus*, 35B,
692 241-254, 1983.

693 Plaza, J., F. J. Gómez-Moreno, L. Núñez, M. Pujadas, and B. Artíñano: Estimation of secondary
694 organic aerosol formation from semi-continuous OC-EC measurements in a Madrid suburban area,
695 *Atmos. Environ.*, 40, 1134-1147, 2006.

696 Polidori, A., B. J. Turpin, H. -J. Lim, J. C. Cabada, R. Subramanian, S. N. Pandis, and A. L. Robinson:
697 Local and regional secondary organic aerosol: insights from a year of semi-continuous carbon
698 measurements at Pittsburgh, *Aerosol Sci. Technol.*, 40, 861-872, 2006.

699 Polissar, A. V., P. K. Hopke, L. Zhou, P. Paatero, S. S. Park, and J. M. Ondov: Atmospheric aerosol
700 over Alaska 2. elemental composition and sources, *J. Geophys. Res.*, 103, 19045-19057, 1998.

701 Reff, A., S. I. Eberly, and P. V. Bhave: Receptor modeling of ambient particulate matter data using
702 Positive Matrix Factorization: review of existing methods, *J. Air Waste Manage. Assoc.*, 57, 146-154,
703 2007.

704 Saylor, R. D., E. S. Edgerton, and B. E. Hartsell: Linear regression techniques for use in the EC tracer
705 method of secondary organic aerosol estimation, *Atmos. Environ.*, 40, 7546-7556, 2006.

706 Schauer, J. J., M. J. Kleeman, G. R. Cass, and B. R. T. Simoneit: Measurement of emissions from air
707 pollution sources. 2. C₁ through C₃₀ organic compounds from medium duty diesel trucks, *Environ. Sci.*
708 *Technol.*, 33, 1578-1587, 1999a.

709 Schauer, J. J., M. J. Kleeman, G. R. Cass, and B. R. T. Simoneit: Measurement of emissions from air
710 pollution sources. 1. C₁ through C₂₉ organic compounds from meat charbroiling, *Environ. Sci.*
711 *Technol.*, 33, 1566-1577, 1999b.

712 Schauer, J. J., M. J. Kleeman, G. R. Cass, and B. R. T. Simoneit: Measurement of emissions from air
713 pollution sources. 5. C₁-C₃₂ organic compounds from gasoline-powered motor vehicles, *Environ. Sci.*
714 *Technol.*, 36, 1169-1180, 2002a.

715 Schauer, J. J., M. J. Kleeman, G. R. Cass, and B. R. T. Simoneit: Measurement of emissions from air
716 pollution sources. 4. C₁-C₂₇ organic compounds from cooking with seed oils, *Environ. Sci. Technol.*,
717 36, 567-575, 2002b.

718 Schauer, J. J., B. T. Mader, J. T. DeMinter, G. Geidemann, M. S. Bae, J. H. Seinfeld, R. C. Flagan, R.
719 A. Cary, D. Smith, B. J. Huebert, T. Bertram, S. Howell, J. T. Kline, P. Quinn, T. Bates, B. Turpin, H.
720 J. Lim, J. Z. Yu, H. Yang, and M. D. Keywood: ACE-Asia intercomparison of a thermal-optical
721 method for the determination of particle-phase organic and elemental carbon, *Environ. Sci. Technol.*,
722 37, 993-1001, 2003.

723 Seila, R. L., H. H. Main, J. L. Arriaga, G. V. Martinez, and A. B. Ramadan: Atmospheric volatile
724 organic compounds measurements during the 1996 Paso del Norte ozone study, *Sci. Total Environ.*,
725 276, 153-169, 2001.

726 Seinfeld, J. H. and S. Pandis: *Atmospheric Chemistry and Physics: From Air Pollution to Climate*
727 *Change*, Wiley, New York, USA, 1998.

728 Stier, P., J. H. Seinfeld, S. Kinne, and O. Boucher: Aerosol absorption and radiative forcing, *Atmos.*
729 *Chem. Phys.*, 7, 5237-5261, 2007.

730 Tsai, W. Y., L. Y. Chan, D. R. Blake, and K. W. Chu: Vehicular fuel composition and atmospheric
731 emissions in South China: Hong Kong, Macau, Guangzhou, and Zhuhai, *Atmos. Chem. Phys.*, 6,
732 3281-3288, 2006.

733 Turpin, B. J., R. A. Cary, and J. J. Huntzicker: An in-situ, time-resolved analyzer for aerosol organic
734 and elemental carbon, *Aerosol Sci. Technol.*, 12, 161-171, 1990.

735 Turpin, B. J. and J. J. Huntzicker: Secondary formation of organic aerosol in the Los-Angeles Basin –
736 a descriptive analysis of organic and elemental carbon concentrations, *Atmos. Environ. Part A*
737 *General Topics*, 25, 207-215, 1991.

738 Turpin, B. J., J. J. Huntzicker, S. M. Larson, and G. R. Cass: Los Angeles mid-day particulate carbon:
739 primary and secondary aerosol, *Environ. Sci. Technol.*, 25, 1788-1793, 1991.

740 Turpin, B. J., J. J. Huntzicker, and S. V. Hering: Investigation of organic aerosol sampling artifacts in
741 the Los Angeles basin, *Atmos. Environ.*, 28, 3061-3071, 1994.

742 Turpin, B. J. and J. J. Huntzicker: Identification of secondary organic aerosol episodes and
743 quantitation of primary and secondary organic aerosol concentrations during SCAQS, *Atmos.*
744 *Environ.*, 29, 3527-2544, 1995.

745 USEPA (Environmental Protection Agency, USA): Health assessment document for diesel engine
746 exhaust, Office of Research and Development, Research Triangle Park, NC, available at:
747 <http://cfpub.epa.gov/ncea/cfm/recordisplay.cfm?deid=29060#Download>, 2002.

748 USEPA (Environmental Protection Agency, USA): Air quality criteria for particulate matter, volumes
749 1 & 2, Office of Research and Development, Research Triangle Park, NC, 2004.

750 Venkatachari, P., L. Zhou, P. K. Hopke, J. J. Schwab, K. L. Demerjian, S. Weimer, O. Hogrefe, D.
751 Felton, and O. Rattigan: An intercomparison of measurement methods for carbonaceous aerosol in the
752 ambient air in New York City, *Aerosol Sci. Technol.*, 40, 788-795, 2006.

753 Wolff, G. T., P. J. Groblicki, S. H. Cadle, and R. J. Countess: Particulate carbon at various locations
754 in the United States, in *Particulate Carbon: Atmospheric Life Cycle*, edited by Wolff. G. T. and R. L.
755 Klimisch, pp.291-315, 1983.

756 Wu, C., W. M. Ng, J. X. Huang, D. Wu, and J. Z. Yu: Determination of elemental and organic carbon
757 in PM_{2.5} in the Pearl River Delta region: inter-instrument (Sunset vs. DRI Model 2011 thermal/optical
758 carbon analyzer) and inter-protocol comparisons (IMPROVE vs. ACE-Asia protocol), *Aerosol Sci.*
759 *Technol.*, 46, 610-621, 2012.

760 Yu, J. Z., J. W. T. Tung, A. W. M. Wu, A. K. H. Lau, P. K. K. Louie, and J. C. H. Fung: Abundance
761 and seasonal characteristics of elemental and organic carbon in Hong Kong PM₁₀, *Atmos. Environ.*,
762 38, 1511-1521, 2004.

763 Yu, X. –Y., R. A. Cary, and N. S. Laulainen: Primary and secondary organic carbon downwind of
764 Mexico City, *Atmos. Chem. Phys.*, 9, 6793-6814, 2009.

765 Yuan, Z. B., J. Z. Yu, A. K. H. Lau, P. K. K. Louie, and J. C. H. Fung: Application of positive matrix
766 factorization in estimating aerosol secondary organic carbon in Hong Kong and its relationship with
767 secondary sulfate, *Atmos. Chem. Phys.*, 6, 25-34, 2006.

768 Zheng, M., G. S. W. Hagler, L. Ke, M. H. Bergin, F. Wang, P. K. K. Louie, L. Salmon, D. W. M. Sin,
769 J. Z. Yu, and J. J. Schauer: Composition and sources of carbonaceous aerosols at three contrasting
770 sites in Hong Kong, *J. Geophys. Res.*, 111, D20313, doi:10.1029/2006JD007074, 2006.

Table 1. Deming regression results of $(OC/EC)_{\min}$ (the slope) and non-combustion term b (the intercept) using the lowest 5% data by OC-to-EC ratio on a monthly, seasonal and annual basis from the one-year carbon measurements at MK AQMS.

Time period	No. of data	λ (Y/X) ¹	$(OC/EC)_{\min}$ (slope) ²	Non-combustion term b (intercept) ²	Correlation coefficient (R^2)
May 2011	34	0.53	0.73 (± 0.025)	0.12 (± 0.190)	0.83
Jun. 2011	24	0.25	0.50 (± 0.035)	-0.29 (± 0.247)	0.64
Jul. 2011	12	0.15	0.38 (± 0.020)	0.18 (± 0.083)	0.95
Aug. 2011	24	0.27	0.52 (± 0.011)	-0.24 (± 0.051)	0.97
Sep. 2011	36	0.29	0.54 (± 0.018)	0.47 (± 0.121)	0.75
Oct. 2011	38	0.54	0.73 (± 0.017)	0.04 (± 0.097)	0.77
Nov. 2011	36	0.49	0.70 (± 0.032)	0.19 (± 0.184)	0.44
Dec. 2011	36	2.14	1.46 (± 0.025)	-0.18 (± 0.161)	0.90
Jan. 2012	38	2.01	1.42 (± 0.046)	-0.58 (± 0.325)	0.70
Feb. 2012	36	0.96	0.98 (± 0.029)	0.25 (± 0.207)	0.93
Mar. 2012	34	0.62	0.78 (± 0.023)	0.61 (± 0.155)	0.85
Apr. 2012	36	0.37	0.61 (± 0.008)	0.32 (± 0.048)	0.88
Summer	94	0.24	0.49 (± 0.003)	-0.20 (± 0.017)	0.90
Fall	72	0.45	0.67 (± 0.011)	0.05 (± 0.065)	0.73
Winter	142	1.02	1.01 (± 0.009)	-0.23 (± 0.062)	0.69
Spring	66	0.45	0.67 (± 0.020)	-0.15 (± 0.134)	0.63
Year	372	0.38	0.62 (± 0.002)	-0.23 (± 0.008)	0.80

¹ $\lambda = \text{Var}(\epsilon_{OC}) / \text{Var}(\epsilon_{EC})$, where $\text{Var}(\epsilon)$ is the variance of the measurement errors, ϵ .

² Values inside parentheses are 95% confidence interval.

Table 2. Deming regression results of $(OC/EC)_{min}$ using subsets of summer EC and OC data varying from the lowest 5% by OC-to-EC ratio to 100%.

Lowest % by OC/EC	No. of data	$(OC/EC)_{min}$ (slope) ¹	Non-combustion term b (intercept) ¹	Correlation coefficient (R ²)
5	94	0.49 (±0.003)	-0.20 (±0.017)	0.90
10	188	0.57 (±0.003)	-0.26 (±0.013)	0.86
20	376	0.66 (±0.002)	-0.26 (±0.009)	0.78
30	564	0.76 (±0.002)	-0.38 (±0.009)	0.72
40	752	0.81 (±0.002)	-0.31 (±0.007)	0.68
50	940	0.88 (±0.001)	-0.32 (±0.007)	0.63
60	1128	0.99 (±0.002)	-0.54 (±0.007)	0.59
70	1316	1.08 (±0.002)	-0.67 (±0.007)	0.55
80	1504	1.19 (±0.002)	-0.80 (±0.007)	0.50
90	1692	1.24 (±0.002)	-0.67 (±0.007)	0.50
100	1878	1.21 (±0.002)	-0.19 (±0.006)	0.33

¹ Values inside parentheses are 95% confidence interval.

Table 3. The average OC-to-EC ratios, calculated as ratio of average OC to average EC, in time periods of 7:00–11:00, 16:00–19:00 and 19:00–22:00 for individual months.

Month	Time period		
	7:00–11:00	16:00–19:00	19:00–22:00
May 2011	0.97	1.22	1.94
Jun. 2011	0.64	0.88	1.45
Jul. 2011	0.56	0.77	1.32
Aug. 2011	0.70	0.82	1.29
Sep. 2011	1.00	1.09	1.88
Oct. 2011	1.27	1.39	2.14
Nov. 2011	1.26	1.32	2.20
Dec. 2011	2.36	2.45	3.66
Jan. 2012	1.90	2.11	3.14
Feb. 2012	1.41	1.77	3.22
Mar. 2012	1.15	1.46	2.35
Apr. 2012	1.04	1.20	1.76

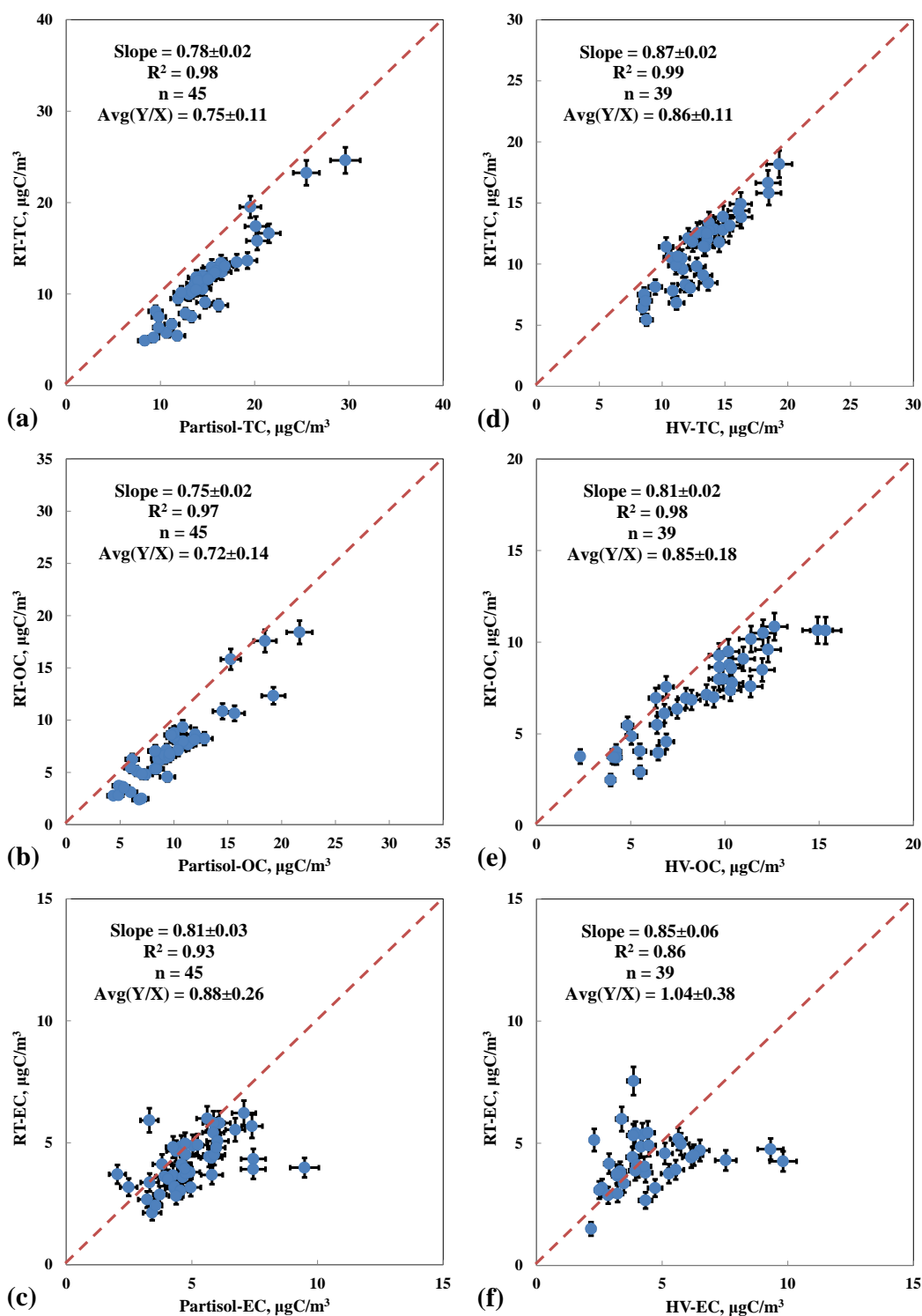


Figure 1. Scatter plots of semi-continuous measurements versus filter-based chemical data for $PM_{2.5}$ samples collected at MK AQMS during May 2011–April 2012. (a) RT-TC vs. Partisol-TC by TOT; (b) RT-OC vs. Partisol-OC by TOT; (c) RT-EC vs. Partisol-EC by TOT; (d) RT-TC vs. HV-TC by TOT; (e) RT-OC vs. HV-OC by TOT and (f) RT-EC vs. HV-EC by TOT.

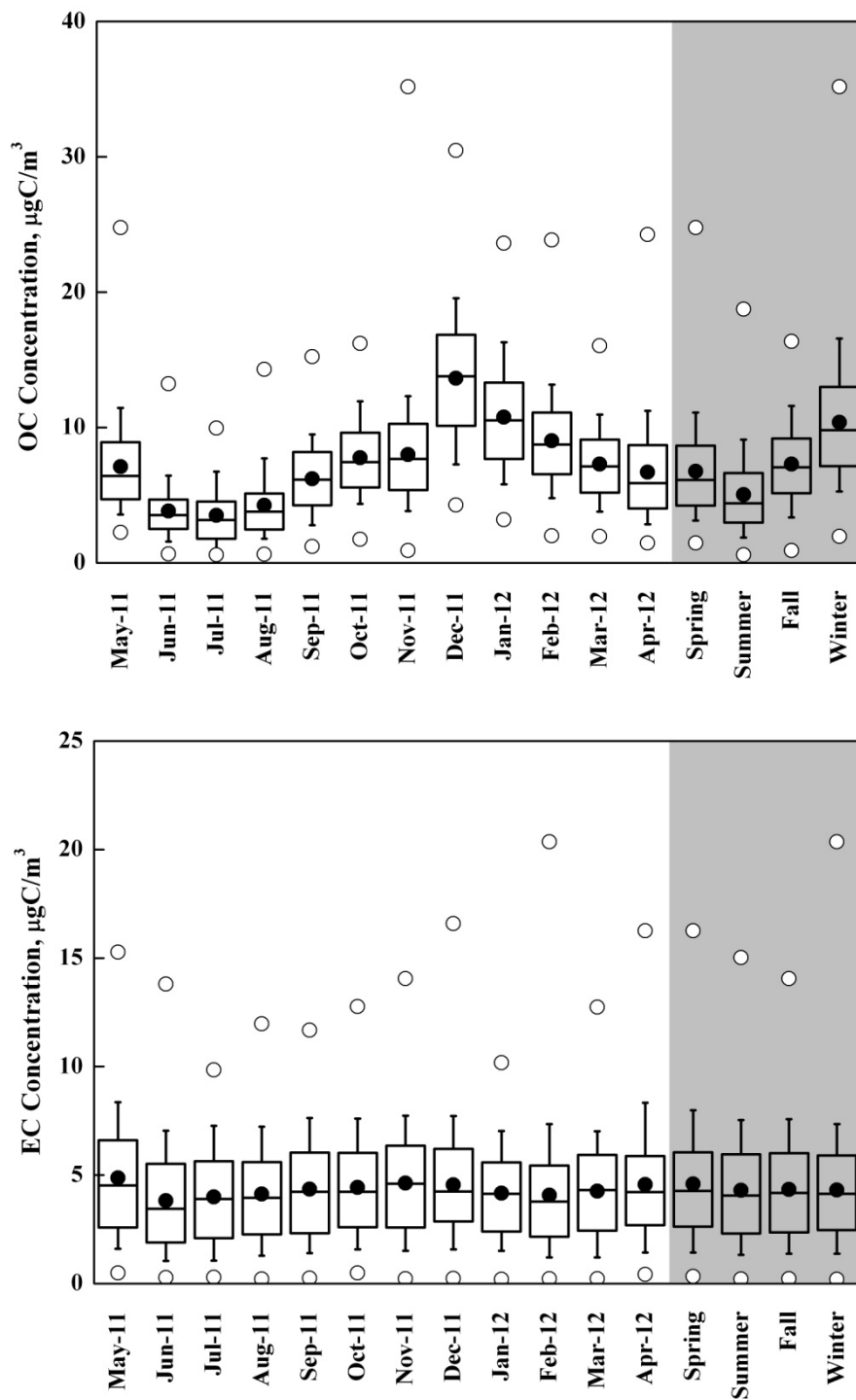


Figure 2. The 1-hr OC and EC concentrations in individual sampling months and in different seasons at MK AQMS during the study period from May 2011 to April 2012 (The box length: the 25th and the 75th percentiles; the whiskers: the 10th and the 90th percentiles; the dot in the box: the average; the line in the box: the median; the circles: the minimum and maximum values).

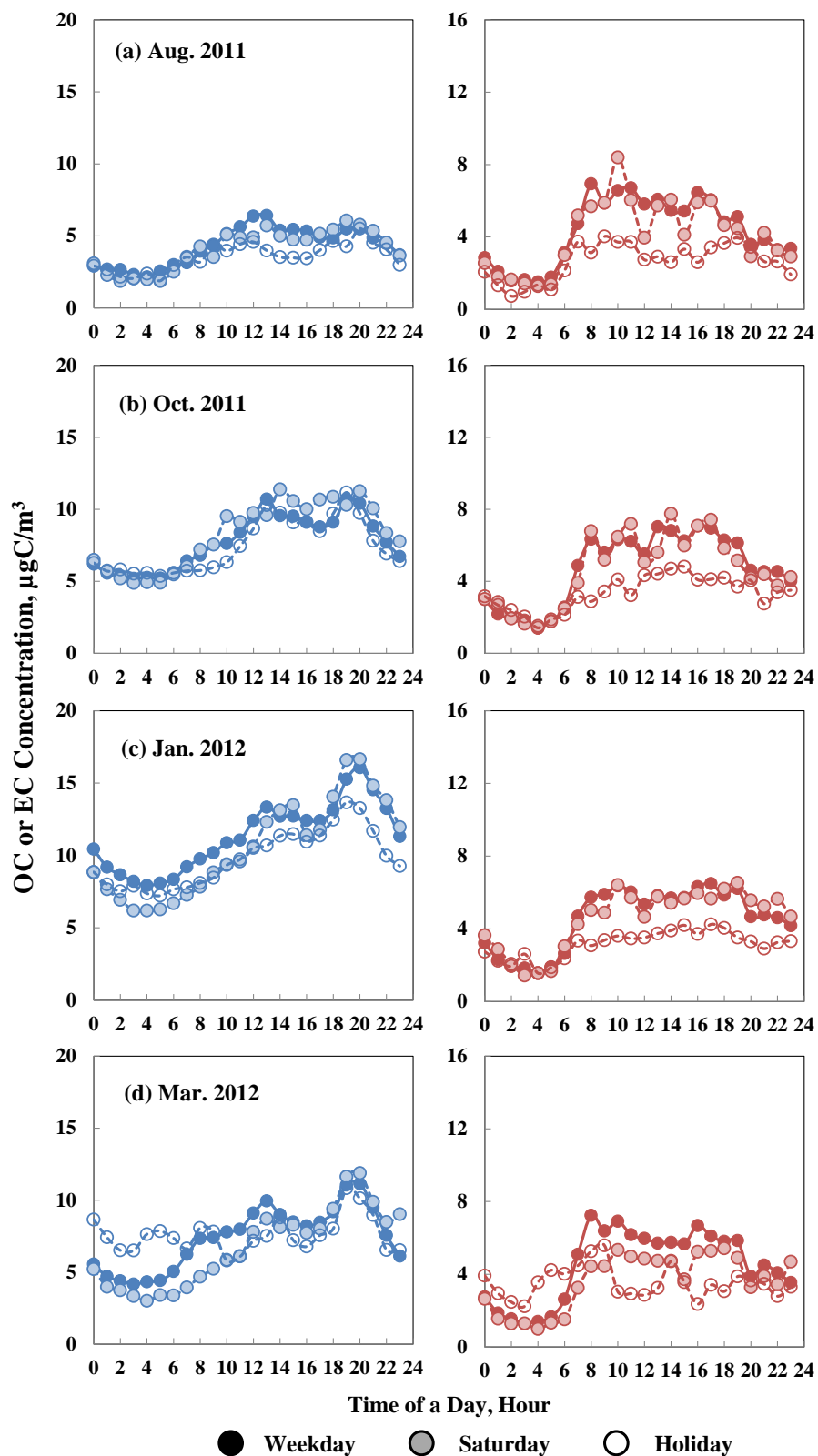


Figure 3. Diurnal variations of OC (blue dots) and EC (red dots) concentrations (unit: $\mu\text{gC}/\text{m}^3$) for weekdays, Saturdays and holidays at MK AQMS in (a) August 2011, (b) October 2011, (c) January 2012 and (d) March 2012.

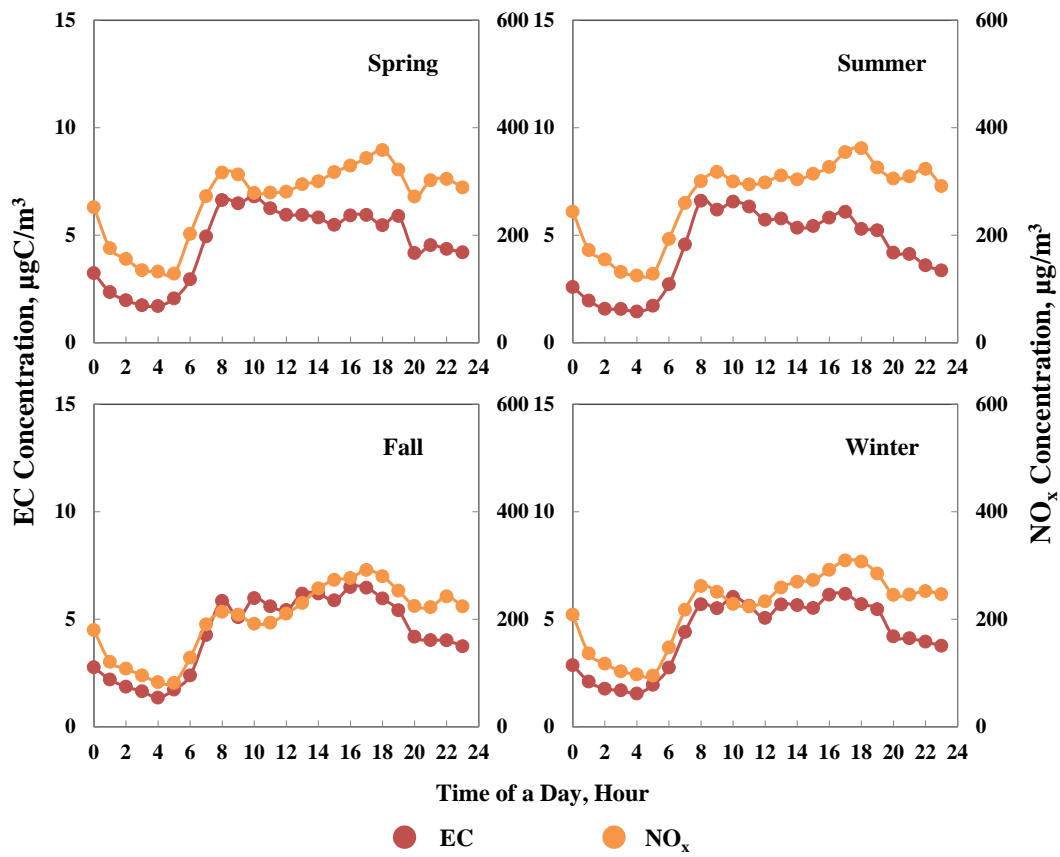


Figure 4. Diurnal variations of EC ($\mu\text{gC}/\text{m}^3$) and NO_x ($\mu\text{g}/\text{m}^3$) at MK AQMS during different seasons.

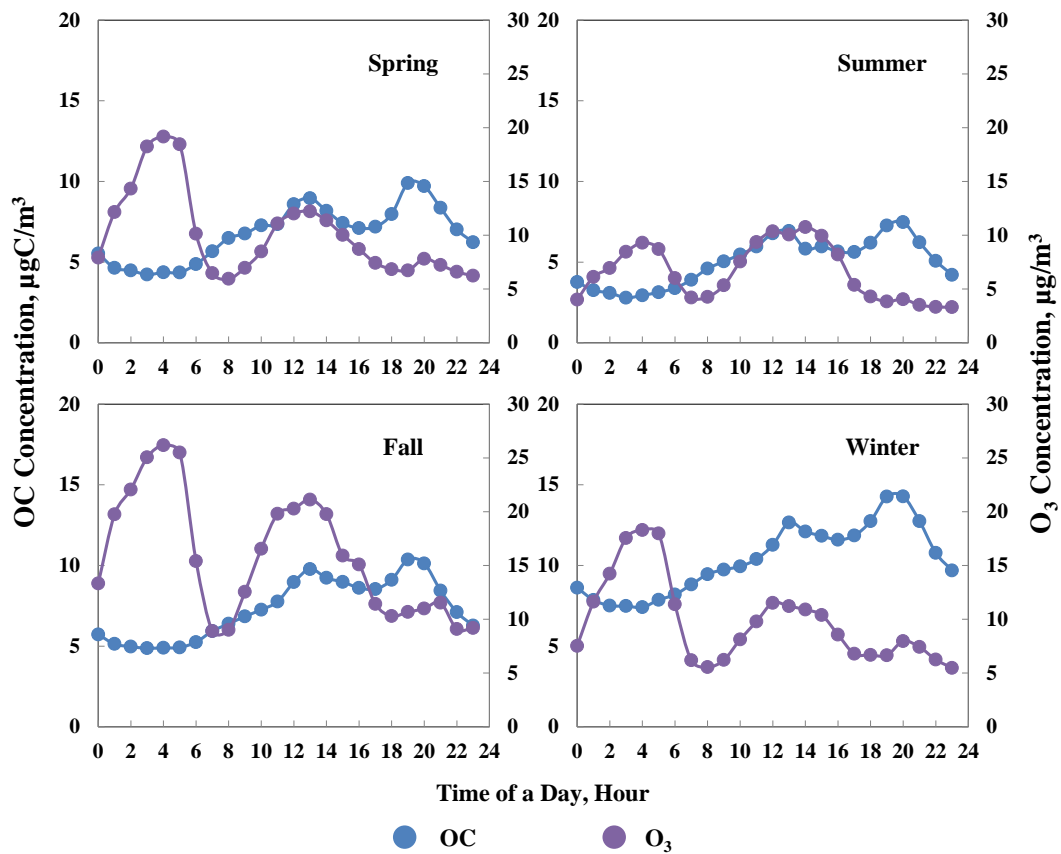


Figure 5. Diurnal variations of OC ($\mu\text{gC}/\text{m}^3$) and O_3 ($\mu\text{g}/\text{m}^3$) at MK AQMS during different seasons. See text for the explanation of the early morning O_3 peak.

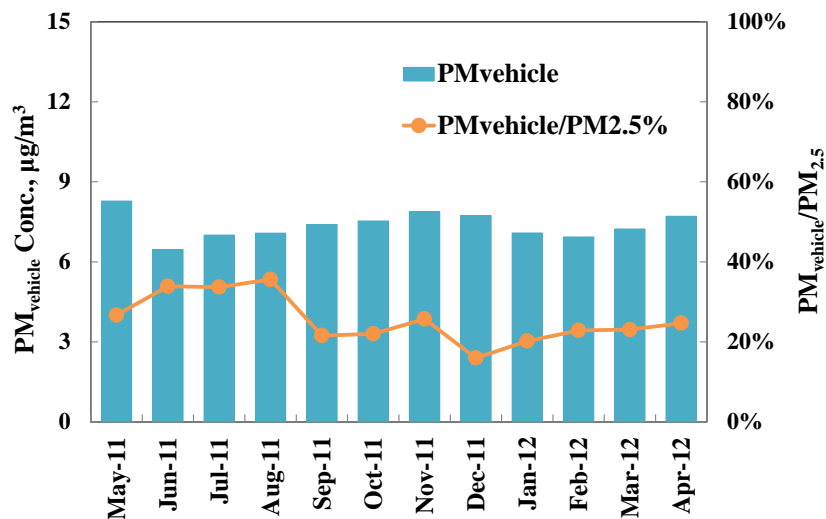


Figure 6. Monthly average vehicle-related $\text{PM}_{2.5}$ concentrations estimated by ($\text{OM}_{\text{vehicle}} + \text{EC}$) and the relative contributions to the monthly average $\text{PM}_{2.5}$ mass at MK AQMS during May 2011–April 2012. (Note: $\text{PM}_{2.5}$ mass concentrations were measured by a Tapered Element Oscillating Microbalance (TEOM 1400AB) on an hourly basis.)

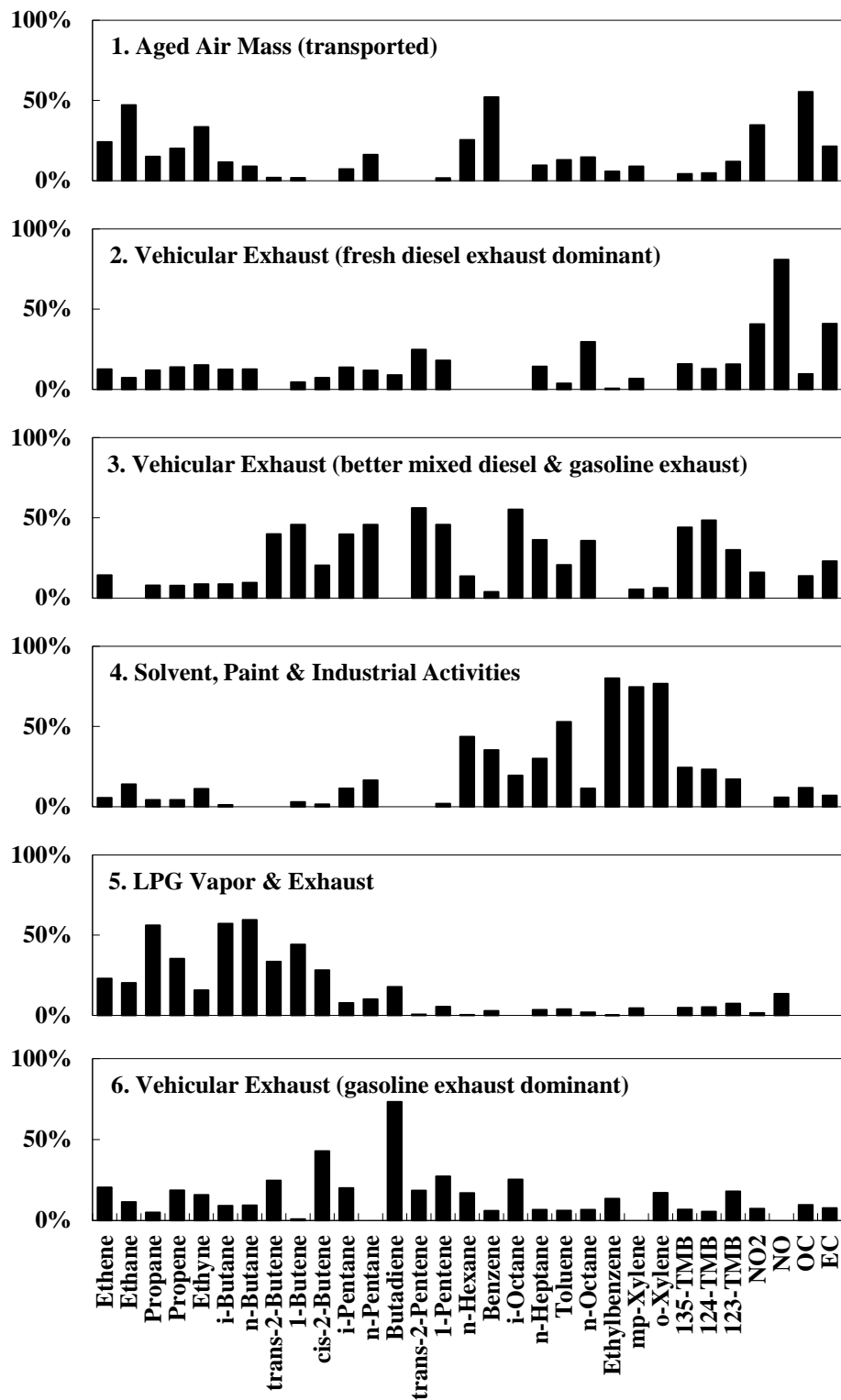


Figure 7. Source profile (% of species total) identified by USEPA PMF3.0.

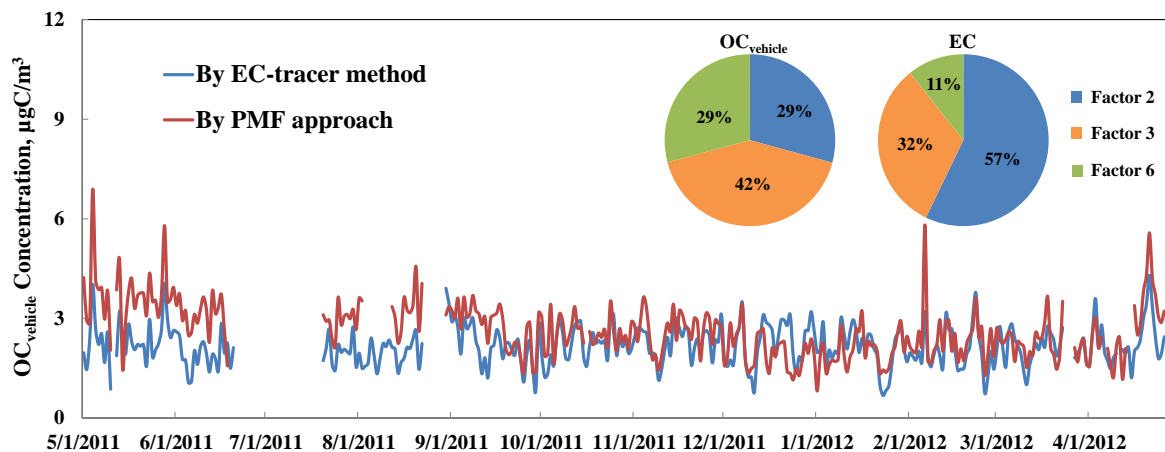


Figure 8. Time-series daily-averaged OC_{vehicle} ($\mu\text{gC}/\text{m}^3$) estimated by EC-tracer method (blue curve) and by PMF approach (red curve) at MK AQMS during May 2011–April 2012. The relative contributions of different vehicular emission-related factors to the OC_{vehicle} and EC, estimated by PMF, are shown in the pie charts.